

Magnetic nanoscale dots on colloid crystal surfaces

S. P. Li, W. S. Lew, Y. B. Xu, A. Hirohata, A. Samad, F. Baker, and J. A. C. Bland

Citation: *Applied Physics Letters* **76**, 748 (2000); doi: 10.1063/1.125882

View online: <http://dx.doi.org/10.1063/1.125882>

View Table of Contents: <http://scitation.aip.org/content/aip/journal/apl/76/6?ver=pdfcov>

Published by the [AIP Publishing](#)

Articles you may be interested in

[An aerosol-mediated magnetic colloid: Study of nickel nanoparticles](#)

J. Appl. Phys. **98**, 054308 (2005); 10.1063/1.2033145

[Printing superparamagnetic colloidal particle arrays on patterned magnetic film](#)

J. Appl. Phys. **93**, 7331 (2003); 10.1063/1.1555908

[Magnetization of ferromagnetic material surfaces by tribological process](#)

J. Appl. Phys. **92**, 6721 (2002); 10.1063/1.1519340

[Effect of surface anisotropy on the hysteretic properties of a magnetic particle](#)

J. Appl. Phys. **91**, 7625 (2002); 10.1063/1.1450846

[Synthesis of monodisperse cobalt nanocrystals and their assembly into magnetic superlattices \(invited\)](#)

J. Appl. Phys. **85**, 4325 (1999); 10.1063/1.370357



Magnetic nanoscale dots on colloid crystal surfaces

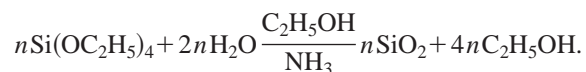
S. P. Li, W. S. Lew, Y. B. Xu, A. Hirohata, A. Samad, F. Baker, and J. A. C. Bland^{a)}
Cavendish Laboratory, University of Cambridge, Cambridge CB3 0HE, United Kingdom

(Received 15 October 1999; accepted for publication 8 December 1999)

We demonstrate that uniform, ordered, single-domain magnetic nanoscale dots can be fabricated on concentrated colloid surfaces. The substrate consists of compact silica nanosphere arrays grown on a glass wafer. Through the subsequent deposition and oxidation treatment of a Co film, monodisperse magnetic Co nanoscale dot arrays with controlled magnetic properties and size were obtained. We suggest that magnetic dots deposited on colloidal surfaces might open a way of developing artificially nanostructured materials for fundamental studies in nanomagnetism and for applications such as patterned magnetic recording media. © 2000 American Institute of Physics. [S0003-6951(00)00106-6]

Templated micro- and nanostructured materials often exhibit special physical properties related to their structural characteristics.¹⁻⁴ For example, inverse opals, templated from opal crystals, are of particular interest as photonic band-gap and electron-transport materials.^{2,3} Hollow-sphere structures produced by colloidal templating are envisioned to have applications in areas ranging from medicine to pharmaceuticals to materials science.⁴ However, there has been a lack of attention focused on the surface of concentrated colloids. By considering a nanoscale periodic solid surface, two promising possibilities arise. First, the periodic surface geometry can be used to fabricate nanostructured materials with periodicities which range from 10 nm to several μm .⁵⁻⁷ Second, the two-dimensional periodic structure can be used to design materials with properties which depend on the artificial dispersion relation (Bloch's theorem).⁸ High-quality concentrated colloids can, in principle, provide such a periodically ordered surface. Here, we describe the use of concentrated colloid surfaces in order to fabricate magnetic nanostructure arrays.

The amorphous silica spheres are synthesized through the hydrolysis of Si alcoxide [tetraethoxysilane (TEOS)], and later polymerization of Si-O chains in ethanol. The net reaction is



The composition of the reactive agents we have chosen is 12 ml TEOS, 30 ml double-distilled water, 7.8 ml ammonium hydroxide (28%), and 150 ml ethanol. Appropriate reaction conditions allow us to obtain perfect spherical microparticles with very small dispersion in diameter (<5%). After diluting the solution with absolute ethanol in the ratio 1:50, the solid structure was formed by natural sedimentation onto a glass wafer. The growth of the crystalline phase leads to a regular and smooth concentrated colloidal surface.⁹⁻¹²

Scanning electron microscopy (SEM) and atomic force microscopy (AFM) were used to assess the surface quality and sphere size. Figure 1 shows a typical SEM photograph of close-packed face-centered-cubic (fcc) silica nanospheres.

The Co film was grown in ultra-high-vacuum conditions (5×10^{-10} mbar) by electron-beam evaporation at normal incidence, as shown in Fig. 2(a). The thickness of Co on the nanosilica spheres should obey $t(\theta) = t_0 \sin \theta$, where t_0 is the thickness of Co on the top of the sphere and θ is the angle with respect to the plane of the sample [Fig. 2(b)]. To obtain separated magnetic dots and to reduce their interaction, controlled oxidation was carried out so that the thinner Co film on the side region of the spheres [i.e., for small θ in Fig. 2(b)] was fully oxidized, thus leaving magnetically isolated Co magnetic dots on the top regions of the spheres. Magnetic force microscopy (MFM) was used to determine the distribution of the Co dots and the magnetic-domain configuration. The magnetization behavior was determined using longitudinal magneto-optical Kerr-effect (MOKE) magnetometry.

Figure 3(a) shows the AFM image of a sample after growing a 10-nm-thick Co film subsequently oxidized in air for three weeks (sample A). A uniform, long-range regular structure in the (111) crystalline plane was found. Figure 3(b) shows a MFM image of this sample. It is clear that separated magnetic dots with the same periodicity as the close-packed silica spheres were formed. The size of the

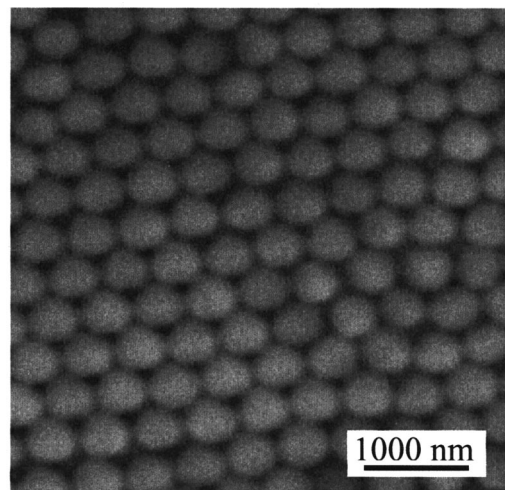


FIG. 1. Typical SEM micrograph of the surface of concentrated silica nanospheres. The image was taken at 40° with respect to the sample surface.

^{a)}Electronic mail: jacbl@phy.cam.ac.uk

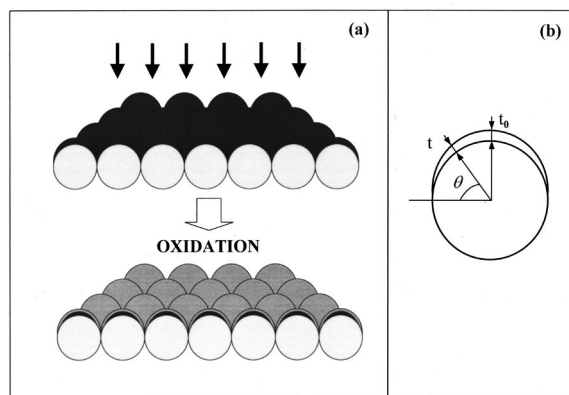


FIG. 2. Schematic diagram of the growing magnetic dots on concentrated silica colloids. (a) Co materials were grown at normal incidence and a subsequent oxidation treatment was carried out after growing. After appropriate oxidation the thinner Co film on the side region of the spheres was fully oxidized, thus leaving magnetically isolated Co magnetic dots on the top regions of the spheres. (b) The thickness dependence of deposited material on the sphere surface for normal direction growth. The thickness t on the nanosilica sphere should obey $t(\theta) = t_0 \sin \theta$, where t_0 is the thickness of the deposited material on the top of the sphere and θ is the angle with respect to the plane of the sample.

magnetic dots is ~ 380 nm with a separation of ~ 100 nm. X-ray photoemission spectroscopy (XPS) measurements performed on a continuous film confirms that the Co layer oxidized in air was approximately 3 nm in thickness. For comparison, we have grown another sample with a composite structure of Cu(5 nm)/Co(20 nm)/SiO₂ spheres (sample B). In this case, the relatively thicker Co film has caused the adjacent Co particles to contact each other, as seen in the MFM image shown in Fig. 3(c). The magnetic structure consists of stripe domains oriented preferably along the $\langle 112 \rangle$ direction of the fcc nanosphere crystal, suggesting that the local dipole fields or symmetry-breaking structures can induce a macroscopic magnetic anisotropy.

The macroscopically smooth sample surface allows us to carry out MOKE measurements with high sensitivity. The most significant features of the hysteresis loops are that samples A and B have different coercivities H_c and saturation magnetic fields H_s [Figs. 4(a) and 4(b)]. The large value of H_c and H_s for sample A is a typical feature of single-domain reversal,¹³ although reversal by a more complicated mechanism cannot be excluded.¹⁴ The relatively small value of H_c and H_s in sample B is likely to be due to domain-wall nucleation and wall motion, which play important roles in this case. However, the barrier for domain-wall propagation along this periodic modulated surface is greater than that for wall motion in a flat continuous film. In order to further understand the magnetic behavior of samples A and B, sample C was prepared for comparison. Sample C was made by growing a Co film on a flat amorphous SiO₂ substrate with the same Co thickness and oxidation treatment as in sample A. Figure 4(c) presents a typical hysteresis loop measured on sample C. The H_s and H_c values of samples A and B are much higher than those of sample C, as expected. For a single-domain dot, the value of the coercivity can be estimated using $H_c \sim 2K_u/M$, where $K_u \sim DM^2/2$, D is a dimensional constant which equals the ratio of thickness (t) to the size (L) of the dots. For sample A, $t \sim 7$ nm, $L \sim 380$ nm, and $M \sim 1.7 \times 10^6$ Oe for Co. The estimated value of H_c

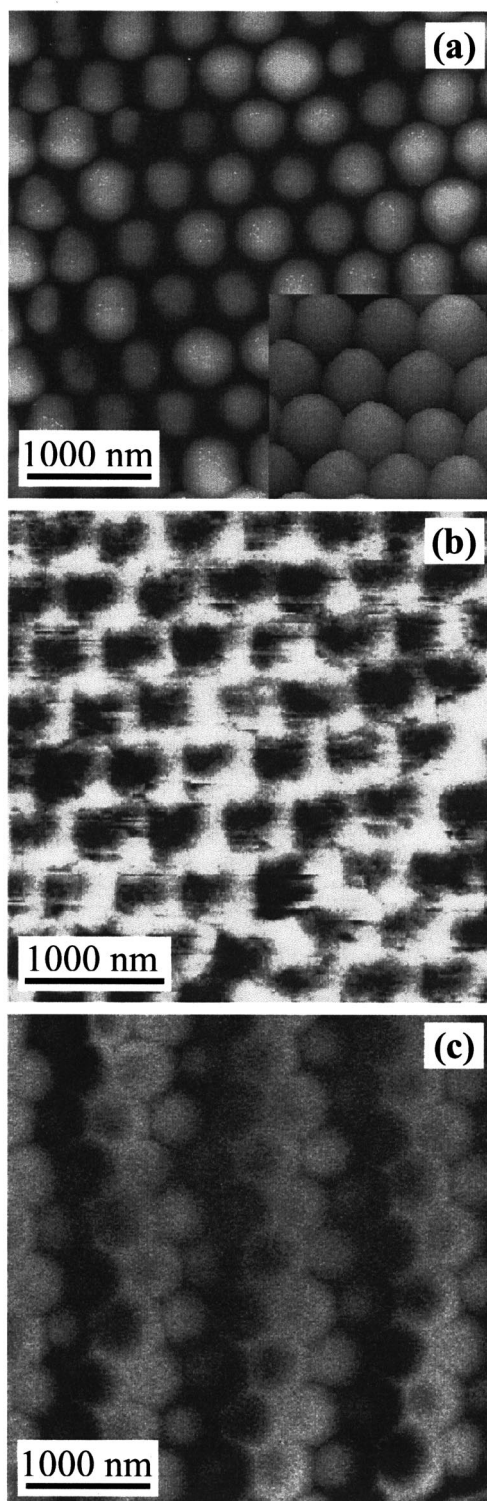


FIG. 3. AFM and MFM images of the concentrated silica colloidal surface after growing the Co film. AFM (a) and MFM (b) images of the sample surface after growing a 10 nm Co film subsequently oxidized in air for three weeks. The separated magnetic Co dots with a long-range periodic structure in the $\langle 111 \rangle$ crystalline plane are seen. In the inset, a three-dimensional AFM image is shown. (c) MFM magnetic-domain image for Cu(5 nm)/Co(20 nm)/SiO₂ spheres. (Here, the 5-nm-thick Cu is a capping layer to prevent oxidation of Co.) The magnetic structure consists of stripe domains due to the relatively thicker Co film and the adjacent Co particles contacted each other.

~ 310 Oe agrees with the experimental value. We have not found a magnetic anisotropy from MOKE measurements in sample B. This is likely to be due to the fact that different crystallites contribute to the signal.

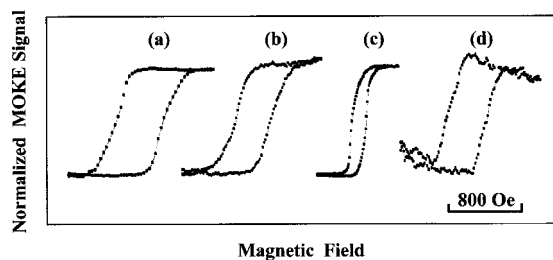


FIG. 4. MOKE hysteresis loops measured on three different samples A, B, and C. (a) Hysteresis loop measured on sample A after growing a 10 nm Co film subsequently oxidized in air for three weeks. (b) Hysteresis loop for Cu 5 nm/Co 20 nm on a silica colloidal substrate. (c) Hysteresis loop measured on Co film growing on a flat amorphous SiO₂ substrate with the same growth and oxidation process as sample A. (d) The last-obtained *in situ* hysteresis loop in thermally oxidized sample A at a heating time of 24 min, after which no MOKE signal was detected. The negative slope of this loop at high field is an experimental artifact.

The large remanence of the hysteresis loop of sample A is an important factor for stable magnetic recording, for example. For thick uncoupled magnetic dots a significant saturation field is expected.^{15,16} However, in our sample the Co dots' thickness is so small that each dot can be viewed as a two-dimensional (2D) magnet. In such 2D cobalt dots the mutual interaction of the dots is negligible, leading to a nearly square hysteresis loop as observed.¹⁷

To give further evidence of the existence of magnetically isolated dots in sample A, we have carried out MOKE measurements on sample A during a thermal oxidation treatment in air (200 °C). This oxidation treatment reduces both the lateral size and the thickness of the cobalt dots. Figure 4(d) shows the hysteresis loop measured at a heating time of 24 min after which no MOKE signal was detected (the sensitivity of MOKE is ~0.5 nm for Co). It shows that there is no

major difference between the loop squareness in Figs. 4(a) and 4(d). Hence, we believe that we have obtained uncoupled 2D magnetic dots in sample A.

In summary, we have demonstrated that concentrated colloid surfaces can be used to fabricate highly uniform, ordered, single-domain magnetic nanoscale dots. The dot size can be controlled by changing the sphere size of the colloids and oxidation process after deposition of magnetic material. Such magnetic arrays allow fundamental studies in nanomagnetism and have potential as structured storage media.

- ¹B. T. Holland, C. F. Blanford, and A. Stein, *Science* **281**, 538 (1998).
- ²V. G. Balakirev, V. N. Bogomolov, and W. Zhuravlev, *Kristallografiya* **38**, 111 (1993) (in Russian).
- ³A. A. Zakhidov, R. H. Baughman, Z. Iqbal, C. Cui, I. Khayrullin, S. O. Dantas, J. Marti, and V. G. Ralchenko, *Science* **282**, 897 (1998).
- ⁴F. Caruso, R. A. Caruso, and H. Möhwald, *Science* **282**, 1111 (1998).
- ⁵A. P. Philipse and A. Vrij, *J. Colloid Interface Sci.* **128**, 121 (1989).
- ⁶P. Pieranski, *Contemp. Phys.* **24**, 25 (1983).
- ⁷N. A. Clark, A. J. Hurd, and B. J. Ackerson, *Nature (London)* **281**, 57 (1979).
- ⁸M. Torres, J. P. Adrados, and F. R. M. de Espinosa, *Nature (London)* **398**, 114 (1999).
- ⁹R. Mayoral, J. Requena, and J. S. Moya, *Adv. Mater.* **9**, 257 (1997).
- ¹⁰R. C. Salvarezza, L. Vázquez, H. Míguez, R. Mayoral, C. López, and F. Meseguer, *Phys. Rev. Lett.* **77**, 4572 (1996).
- ¹¹H. Míguez, C. López, F. Meseguer, A. Blanco, L. Vázquez, R. Mayoral, M. Ocaña, V. Fornés, and A. Mifsud, *Appl. Phys. Lett.* **71**, 1148 (1997).
- ¹²A. van Blaaderen, R. Ruel, and P. Wiltzius, *Nature (London)* **385**, 321 (1997).
- ¹³E. C. Stoner and E. P. Wohlfarth, *Proc. R. Soc. London, Ser. A* **240**, 599 (1948).
- ¹⁴M. S. Lederman and M. Ozaki, *Phys. Rev. Lett.* **73**, 1986 (1994).
- ¹⁵J. F. Smyth, S. Schultz, D. Kern, H. Schmid, and D. Yee, *J. Appl. Phys.* **63**, 4237 (1988).
- ¹⁶M. Hehn, K. Ounadjela, J. P. Bucher, F. Rousseaux, D. Decanini, B. Bartenlian, and C. Chappert, *Science* **272**, 1782 (1996).
- ¹⁷C. Stamm, F. Marty, A. Vaterlaus, V. Weich, S. Egger, U. Maier, U. Ramsperger, H. Fuhrmann, and S. Pescia, *Science* **282**, 449 (1998).